Journal of Fluorine Chemistry 131 (2010) 1122–1132

Contents lists available at ScienceDirect

Journal of Fluorine Chemistry

journal homepage: www.elsevier.com/locate/fluor

Mechanistic investigation of vinylic carbon–fluorine bond activation of perfluorinated cycloalkenes using $Cp^*_2ZrH_2$ and Cp^*_2ZrHF

Bradley M. Kraft [a], Eric Clot [b], Odile Eisenstein [b], William W. Brennessel [c], William D. Jones [c,*]

[a] St. John Fisher College, 3690 East Avenue, Rochester, NY 14618, United States
[b] Institut Charles Gerhardt, Université Montpellier 2, CNRS 5253, Case Courrier 1501, Place E. Bataillon, 34095 Montpellier, France
[c] Department of Chemistry, University of Rochester, Rochester, NY 14627, United States

ARTICLE INFO

Article history:
Received 26 March 2010
Received in revised form 13 May 2010
Accepted 14 May 2010
Available online 2 July 2010

Keywords:
Perfluorocyclobutene
Zirconium
C–F bond activation
Insertion
Metathesis
DFT

This article is dedicated to Russ Hughes in honor of his receipt of the 2010 ACS Award for Creative Work in Fluorine Chemistry.

ABSTRACT

$Cp^*_2ZrH_2$ (**1**) (Cp^*: pentamethylcyclopentadienyl) reacts with cyclic perfluorinated olefins to give Cp^*_2ZrHF (**2**) and hydrodefluorinated products under very mild conditions. Initial C–F bond activation occurs selectively at the vinylic positions of the cycloolefin to exchange fluorine for hydrogen. Several mechanisms are discussed for this H/F exchange: (a) olefin insertion/β-fluoride elimination, (b) olefin insertion/α-fluoride elimination, and (c) hydride/fluoride σ-bond metathesis. Following H/F σ-bond metathesis exchange of both vinylic C–F bonds of perfluorocyclobutene, **1** then reacts with allylic C–F bonds by insertion/β-fluoride elimination. A similar sequence is observed with perfluorocyclopentene. Cp^*_2ZrHF reacts selectively with vinylic C–F bonds of perfluorocyclobutene to give 3,3,4,4-tetrafluorocyclobutene and $Cp^*_2ZrF_2$ without further hydrodefluorination occurring. In the presence of excess **1** and H_2, perfluorocyclobutene and perfluorocyclopentene are reduced to cyclobutane and cyclopentane in 46% and 16% yield, respectively. DFT calculations exclude the pathway by way of the olefin insertion/α-fluoride elimination and suggest that the pathway by way of hydride/fluoride σ-bond metathesis is preferred.

1. Introduction

The activation of carbon–fluorine bonds remains a challenging goal due to the high strength of these bonds and the small size and high electronegativity of the fluorine atom [1]. Fluorine has found important applications in materials ranging from Teflon and refrigerants to pharmaceuticals and agrochemicals. The use of transition metal complexes to break C–F bonds in highly fluorinated organic molecules has been targeted as a means of selectively introducing partial fluorination in a product [2].

The activation of aromatic sp^2 C–F bonds has been seen with many transition metal complexes, and a variety of mechanisms have been proposed. For example, $Ru(dmpe)_2H_2$ reacts with C_6F_6 to give HF and $Ru(dmpe)_2(C_6F_5)H$ by way of initial electron transfer from ruthenium to hexafluorobenzene [3]. $Pt(PCy_3)_2H_2$ behaves similarly [4]. In contrast, $Cp^*Rh(PMe_3)H_2$ reacts with C_6F_6 by way of an S_NAr2 attack by its conjugate base to give $Cp^*Rh(PMe_3)(C_6F_5)H$ and fluoride ion, resulting in an autocatalytic reaction [5]. $Cp^*Ir(CO)_2$ is also proposed to react with C_6F_6 via an S_NAr2 mechanism [6]. $Ni(PEt_3)_4$ reacts with hexafluorobenzene via oxidative addition to give $Ni(PEt_3)_2(C_6F_5)F$ [7]. Photochemically induced C–F activation occurs in the complex $Cp^*Rh(PMe_3)(\eta^2\text{-}C_6F_6)$ to give $Cp^*Rh(PMe_3)(C_6F_5)F$ [8].

Examples of sp^2 C–F activations of perfluorinated alkenes by transition metal complexes are more rare. The metal carbonyl anions $[(\eta^5\text{-}C_5R_5)M(CO)_2]^-$ (M = Fe, R = H; M = Fe, R = CH_3; M = Ru, R = H) react with octafluorocyclooctatetraene (OFCOT) to afford monosubstitution products via nucleophilic displacement of fluoride ion, which then undergo an intramolecular cyclization (Eq. (1)) [9]. $Me_3Sn\text{–}Mn(CO)_5$ reacts with $CF_2{=}CFH$ upon photolysis to produce $CHF{=}CFMn(CO)_5$ and Me_3SnF. A mechanism involving olefin insertion to give $Me_3SnCFHCF_2Mn(CO)_5$ followed by fluoride migration was proposed to give the observed

* Corresponding author at: Department of Chemistry, University of Rochester, Hutchison Hall, Rochester, NY 14627, United States. Tel.: +1 585 275 5493; fax: +1 585 276 0011.
E-mail address: jones@chem.rochester.edu (W.D. Jones).

0022-1139/$ – see front matter © 2010 Elsevier B.V. All rights reserved.
doi:10.1016/j.jfluchem.2010.05.003

products [10].

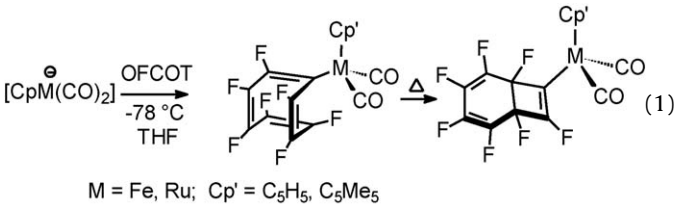

$Cr(\eta^6\text{-}C_6H_6)_2$ has been shown to oligomerize perfluoropropene to give a mixture of perfluorodimers and trimers following loss of a C_6H_6 ligand (Eq. (2)) [11]. Many other reports of perfluoroolefin oligomerization or isomerization involve generation of a perfluorocarbanion using a source of fluoride ion [12].

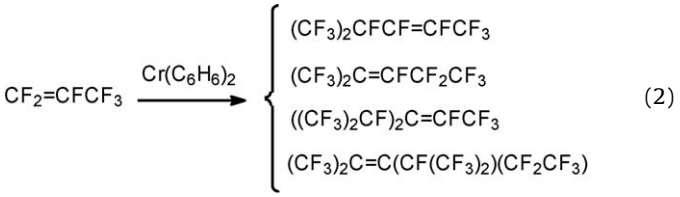

A few organometallic hydrides have been reported to react with perfluoroalkenes, leading to C–F activated products. $CpM(CO)_3H$ (M = Mo, W) reacts with $CF_2{=}CF_2$ to afford insertion products $CpM(CO)_3(CF_2CF_2H)$ in about 70% yield, but no β-fluoride elimination occurs [13]. In contrast, $Mn(CO)_5H$ reacts similarly to give $Mn(CO)_5(CF_2CF_2H)$, but decomposes upon heating at 150 °C to release $CF_2{=}CFH$, $CF_2{=}CH_2$, and CO [14]. Surprisingly, olefin insertion only occurred with $CF_2{=}CF_2$ and not with olefins such as $CF_2{=}CH_2$, $CF_2{=}CHCl$, $CF_2{=}CF{-}CF_3$, or (*Z*)-$CF_3CF{=}CFCF_3$. Braun has observed the reaction of perfluoropropene with $RhH(PEt_3)_3$ and base to yield $Rh(CF{=}CFCF_3)(PEt_3)_3$ in 80% yield [15]. Whittlesey has seen multiple hydride/fluoride exchanges between $Ru(dmpe)_2H_2$ and perfluoropropene or $(CF_3)_2C{=}C(F)CF_2CF_3$ [16]. Recently, Lentz reported the use of Cp_2TiF_2 as a *catalyst* for H/F exchange between perfluoropropene and silanes [17].

Our group has been interested in the reactions of $Cp^*_2ZrH_2$ (**1**) with a wide variety of fluorocarbon substrates. $Cp^*_2ZrH_2$ reacts with C_6F_6 to give a 1:1 mixture of $Cp^*_2Zr(C_6F_5)H$ and C_6F_5H, along with a stoichiometric quantity of Cp^*_2ZrHF (**2**) [18]. Aliphatic fluorocarbons react to form Cp^*_2ZrHF and alkane by a radical chain mechanism [19]. Fluorobenzene reacts with $Cp^*_2ZrH_2$ to form benzene, Cp^*_2ZrHF, and $Cp^*_2Zr(C_6H_5)F$ via competing dual mechanisms involving (1) hydride/fluoride σ-bond metathesis and (2) initial ortho C–H activation, β-F elimination to give an intermediate benzyne complex, and insertion of the coordinated benzyne into the Zr–H bond [19b,20]. Non-fluorinated alkenes containing perfluoroalkyl substituents such as 3,3,3-trifluoropropene or $CH_2{=}CHCF_2CF_2CF_2CF_3$ react by olefin insertion into the Zr–H bond (both regioisomers) followed by reductive elimination to give a fluoroalkane or β-fluoride elimination to give fluoroolefins (Scheme 1) [21].

$Cp^*_2ZrH_2$ has been found to hydrodefluorinate perfluorinated alkenes to afford Cp^*_2ZrHF and hydrodefluorinated organic products [22]. Unlike 3,3,3-trifluoropropene no intermediates were observed at low temperature. The mechanism for these reactions was established to involve olefin insertion/β-fluoride elimination by DFT calculations using Cp as a model for Cp*. As shown in Eq. (3), reaction of 1 equiv. of $Cp^*_2ZrH_2$ (**1**) with perfluoropropene yields primarily (*E*)-$CF_3CF{=}CHF$ and Cp^*_2ZrHF (**2**). Subsequent addition of additional equivalents of **1** produced $Cp^*_2Zr(CH_2CH_2CH_3)H$, which eliminated propane. Cp^*_2ZrHF was also found to react selectively with perfluoropropene to give (*E*)-$CFH{=}CFCF_3$ and $Cp^*_2ZrF_2$, but further hydrodefluorination was not

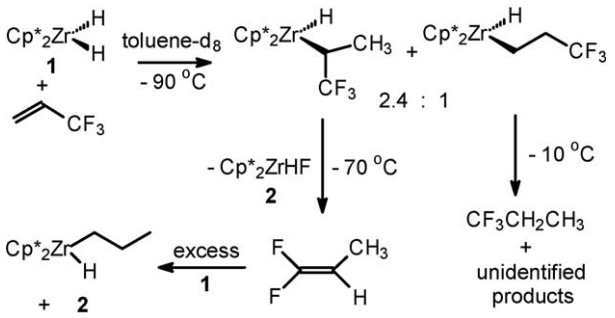

Scheme 1. Reaction of $Cp^*_2ZrH_2$ with trifluoropropene (from Ref. [21], used with permission).

observed. A summary of the various mechanisms for C–F cleavage by $Cp^*_2ZrH_2$ has been reported [23].

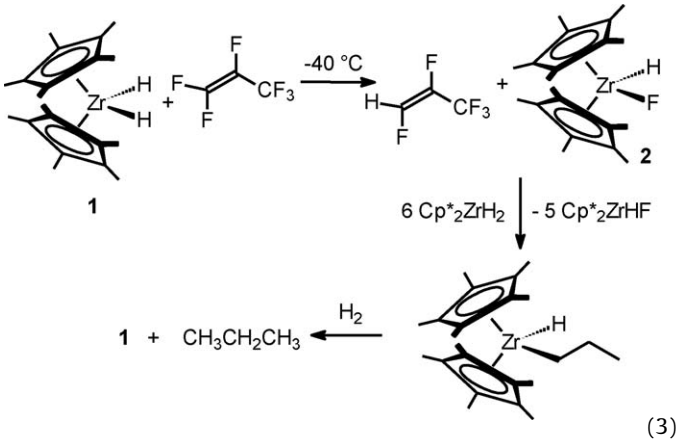

Here, we report related reactions of $Cp^*_2ZrH_2$ with two perfluorocycloolefins, perfluorocyclobutene and perfluorocyclopentene. Perfluoroolefins are unique in that they are extremely susceptible to attack by nucleophiles [24]. Careful examination of the course of the reaction reveals vinylic hydrodefluorination

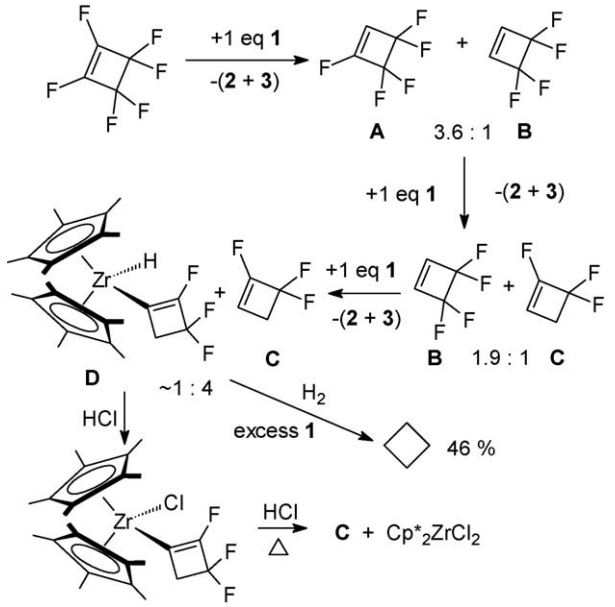

Scheme 2. Stepwise defluorination of perfluorocyclobutene by $Cp^*_2ZrH_2$.

products that *cannot be accommodated* by an olefin insertion/β-fluoride elimination pathway. Once the olefinic fluorines are replaced by hydrogen to generate non-fluorinated olefins, however, further reaction does proceed by olefin insertion/β-fluoride elimination.

2. Results and discussion

2.1. Reaction of perfluorocyclobutene and $Cp^*_2ZrH_2$

Reaction of perfluorocyclobutene (1 equiv.) with $Cp^*_2ZrH_2$ (**1**) at room temperature forms a mixture of vinylic C–F activated products, 1,3,3,4,4-pentafluorocyclobutene (**A**) and 3,3,4,4-tetrafluorocyclobutene (**B**) in 3.6:1 ratio. Both Cp^*_2ZrHF (**2**) and $Cp^*_2ZrF_2$ (**3**) are observed in approximately 1:2 ratio (Scheme 2). Independent experiments demonstrate that $Cp^*_2ZrF_2$ is formed by secondary reaction of Cp^*_2ZrHF with perfluorocyclobutene. The reaction with **1** in toluene-d_8 was found to occur below −70 °C and no intermediates could be observed using low temperature NMR spectroscopy. Addition of a subsequent equivalent of **1** to the mixture of **A** and **B** produced **2**, a trace of $Cp^*_2ZrF_2$, and a 1.9:1 mixture of **B** and 1,4,4-trifluorocyclobutene (**C**), the allylic C–F activated product of **B**. Addition of a third equivalent of $Cp^*_2ZrH_2$ resulted in formation of **C**, $Cp^*_2Zr(c\text{-}C_4F_3H_2)H$ (**D**), and cyclobutane in 17:4:1 ratio plus **2** and H_2. All fluoroolefin products were characterized by ^1H, ^{19}F, ^1H COSY, ^{19}F COSY NMR spectroscopy, and GC/MS. Complex **D** was characterized by ^1H, ^{19}F, and ^{19}F COSY NMR only, as this complex was elusive to separation and independent preparation. Addition of anhydrous HCl to the reaction mixture containing **D** produced $Cp^*_2Zr(c\text{-}C_4F_3H_2)Cl$ and H_2. Heating $Cp^*_2Zr(c\text{-}C_4F_3H_2)Cl$ at 80 °C with excess HCl produced $Cp^*_2ZrCl_2$ and olefin **C**. In a separate experiment employing an internal standard, reaction of excess **1** with perfluorocyclobutene in the presence of 1.3 atm H_2 ultimately afforded a 46% yield (NMR) of cyclobutane.

Reaction of 1 equiv Cp^*_2ZrHF (**2**) with perfluorocyclobutene produced a mixture of olefin **A**, **B** and $Cp^*_2ZrF_2$ (**3**) within 2 h at room temperature. In the presence of an additional equivalent of **2**, olefin **B** and **3** are formed quantitatively (Eq. (4)). In the presence of excess **2**, no further hydrodefluorination was observed, even with heating at 85 °C for 3 h.

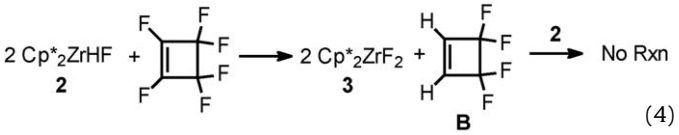

(4)

2.2. Reaction of perfluorocyclopentene and $Cp^*_2ZrH_2$

Reaction of perfluorocyclopentene (1 equiv.) with **1** at room temperature forms a mixture of the vinylic and aliphatic C–F activated products, 1,3,3,4,4,5,5-heptafluorocyclopentene (**E**) and 1,2,3,3,4,5,5-heptafluorocyclopentene (**F**) in 2.6:1 ratio along with **2** and **3** (Scheme 3). Independent experiments show that **2** reacts with perfluorocyclopentene over ~1 day at room temperature to give a mixture of olefin **E**, 3,3,4,4,5,5-hexafluorocyclopentene (**G**), and **3** with no formation of olefin **F**.

Monitoring the reaction with **1** by NMR spectroscopy at low temperature, **E** and **F** were formed at −50 °C and no intermediates could be detected. A slight improvement in selectivity was observed under these conditions, producing **E** and **F** in 4:1 ratio. When 3 additional equivalents of **1** were added to the mixture of **E** and **F**, both olefin **G** and 1,4,4,5,5-pentafluorocyclopentene (**H**) were observed (1:16) in addition to unreacted **E** and **F**. Addition of

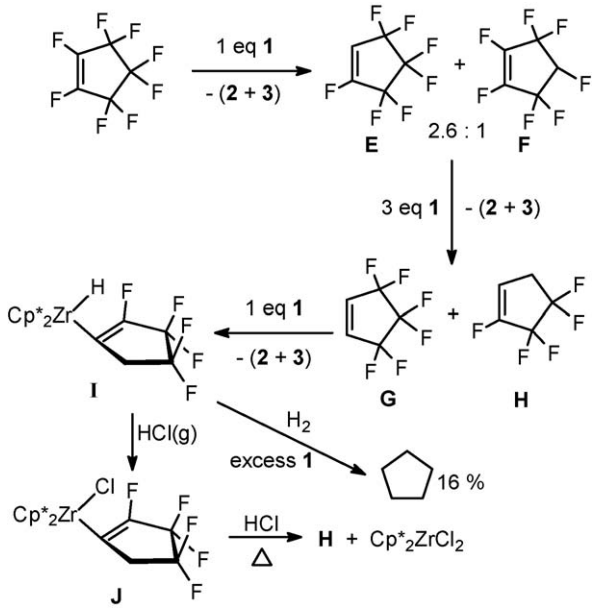

Scheme 3. Stepwise defluorination of perfluorocyclopentene by $Cp^*_2ZrH_2$.

excess **1** to this mixture forms primarily olefin **H**, and traces of a few other unidentified volatile fluorinated species. Olefin **H** reacts with **1** at room temperature to give $Cp^*_2Zr(c\text{-}C_5F_5H_2)H$ (**I**) with ~10% increase in **2**. Complex **I** was isolated cleanly in 42% yield (based on perfluorocyclopentene) and has been fully characterized by ^1H, ^{19}F, ^{19}F COSY NMR spectroscopy, and elemental analysis. **I** reacts quantitatively with 1 equiv of anhydrous HCl at room temperature to form $Cp^*_2Zr(c\text{-}C_5F_5H_2)Cl$ (**J**) and H_2. The X-ray structure of **J** is shown in Fig. 1.

Thermolysis of **J** at 80 °C in the presence of excess HCl forms $Cp^*_2ZrCl_2$ and olefin **H**. **H** was characterized by ^1H and ^{19}F NMR spectroscopy, GC/MS, and derivatization by hydrogenation to give 1,1,2,2,3-pentafluorocyclopentane. Thermolysis of **I** in the presence of excess **1** and 1.3 atm H_2 forms **2**, cyclopentane, and other unidentified products. Cyclopentane was observed in only 16% yield by NMR integration, based on perfluorocyclopentene.

Of all of the fluoroolefin products observed, olefin **F** is most unexpected as it involves reduction of an isolated aliphatic C–F bond. A radical abstraction of fluorine by $Cp^*_2Zr^{III}H$ seems likely for the formation of olefin **F** as aliphatic C–F activation has been shown

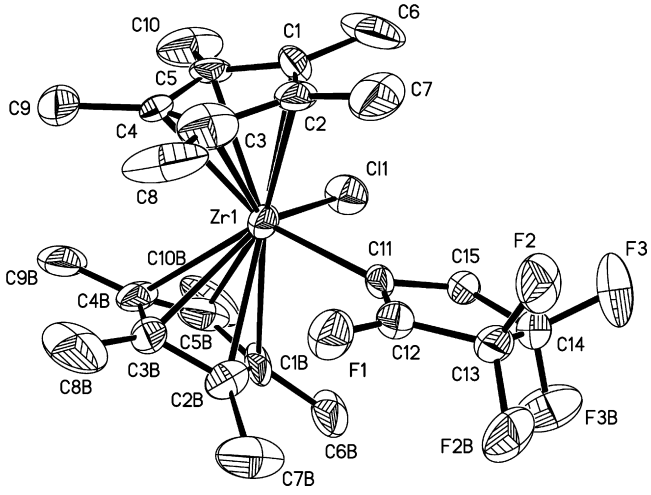

Fig. 1. ORTEP drawing of $Cp^*_2Zr(c\text{-}C_5F_5H_2)Cl$, **J**, showing 50% probability ellipsoids.

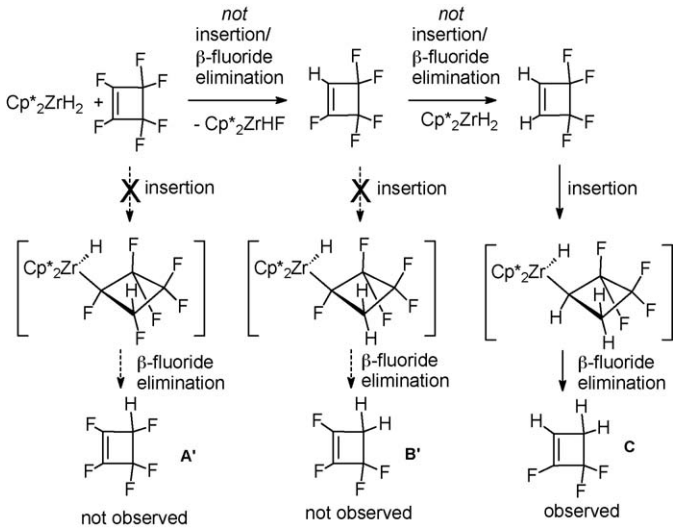

Scheme 4. Pathways for C–F activation.

to occur by this mechanism, although more harsh conditions would be expected [19]. In an attempt to hinder the formation of **F** by a radical pathway, the reaction was repeated in the presence of the radical inhibitor, triphenylmethane (10 equiv), but no change was observed in the ratio of olefins **E** and **F**. It might be possible that the opposing double bond directs the C–F activation in an as yet unidentified fashion.

2.3. Exchange of vinylic C–F bonds: olefin insertion/β-fluoride elimination

As mentioned earlier, C–F bond activation reactions with olefins such as 3,3,3-trifluoropropene and 1,1-difluoroethylene have been shown to produce Cp^*_2ZrHF and hydrodefluorinated organic products by insertion/β-fluoride elimination [21]. This mechanism is also conceivable in the initial reaction of **1** with perfluoropropene at low temperature to give (*E*)-CFH=CF–CF_3, via the isopropyl hydride intermediate, $Cp^*_2Zr[(CF(CF_3)(CF_2H))]H$, prior to selective β-F elimination. However, the reactions with cyclic perfluorinated olefins suggest that this mechanism is not possible for this vinylic C–F activation reaction, as discussed below.

Insertion reactions by metal hydrides are well known to occur via cis addition of the M–H bond across the double bond [25]. Insertion of a cyclic perfluorinated olefin with **1** would be expected to therefore lead to a cyclobutyl hydride complex with only one fluorine atom accessible for β-F elimination (Scheme 4). The cis addition forces the other fluorine atoms on the β carbons to the opposite face of the ring. β-fluoride elimination would also be expected to occur by cis-elimination [26]. It is clear that β-F elimination is *not occurring* in the vinylic H/F exchange reactions to produce **A** and **B** as β-F elimination from this cyclobutyl hydride intermediate would give the allylic C–F activated products **A′** and **B′**, but this is not observed experimentally. The formation of **C**, however, can be explained via insertion/β-fluoride elimination. In fact, earlier studies of non-cyclic non-perfluoroolefins showed evidence for this exact pathway, as the alkyl hydride intermediates with β-fluorines could be observed at low temperature [21].

2.4. Exchange of vinylic C–F bonds: olefin insertion/α-fluoride elimination

Another possible mechanism to explain the vinylic C–F activation products would be to still begin with olefin insertion, but then follow with α-fluoride elimination from the cyclobutyl hydride complex to give **2** and a fluorocarbene (Scheme 5). The fluorocarbene could then quickly insert into the adjacent C–H bond to give the observed H/F substitution at the vinylic carbon.

To examine the possibility of α-fluoride elimination, the complex $Cp^*_2ZrH_2$ was reacted with $Hg(CF_3)_2$ in an attempt to make $Cp^*_2ZrH(CF_3)$ [27]. Evolution of a gas (H_2) and formation of Hg^0 was observed. ^1H and ^{19}F NMR spectroscopy showed the formation of **2**, **3**, and traces of CH_3F, CH_4, and C_2H_6. When the reaction was repeated in the presence of tetramethylethylene, a known carbene trap [28], 1-fluoro-2,2,3,3-tetramethylcyclopropane was observed, but not 1,2-difluoro-2,2,3,3-tetramethylcyclopropane. This observation can be accommodated by the sequence shown in Eq. (5). If a CF_3 group is transferred by $Hg(CF_3)_2$ to zirconium, α-fluoride elimination would generate a

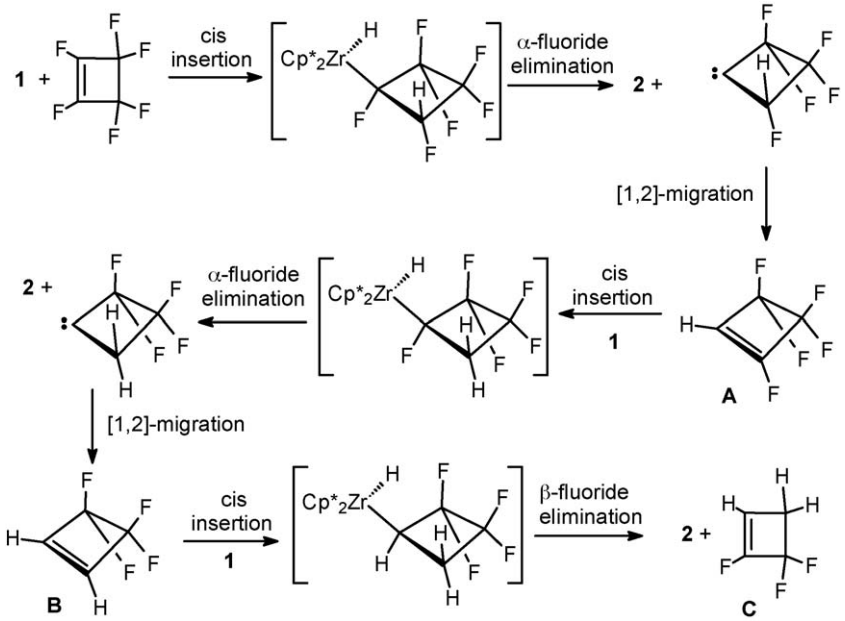

Scheme 5. α-Elimination pathway for C–F activation.

carbene species $Cp^*_2ZrHF(=CF_2)$, which could then insert into the Zr–H bond to produce $Cp^*_2Zr(CF_2H)F$. A second α-fluoride elimination would maximize the number of Zr–F bonds, producing **3** and free:CFH, which could then be trapped to give the observed monofluorocyclopropane product.

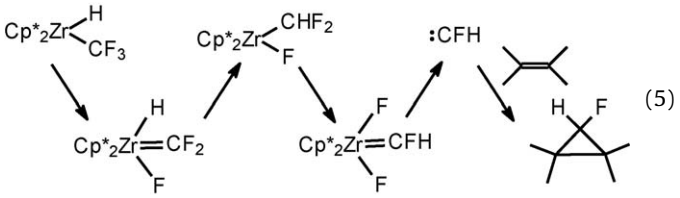

(5)

There is a precedent that α-F elimination processes in zirconocene complexes may be facile. Morrison has shown that $Cp^*_2ZrCl_2$ reacts with $Cd(CF_3)_2$·DME at −25 °C to give $Cp^*_2ZrF_2$ in 91% isolated yield [29]. The species $Cp^*_2Zr(CF_3)_2$ was proposed as an intermediate. In contrast, the complex $Cp_2TiF(CF_3)$ has been synthesized and isolated, and is very stable in solution, so that it appears that not all group 4 complexes are prone to α-fluoride elimination [30]. An α-fluoride elimination pathway with perfluorocycloolefins remains as a possible mechanism for vinylic C–F exchange.

2.5. Exchange of vinylic C–F bonds: hydride/fluoride σ-bond metathesis

Vinylic H/F exchange in perfluorinated olefins by $Cp^*_2ZrH_2$ and Cp^*_2ZrHF may also be explained by a nucleophilic hydride addition to the double bond to give an intermediate carbanion followed by subsequent fluoride elimination to form a Zr–F bond (Eq. (6)). Alternatively, the mechanism may be viewed as a 4-electron-4-centered σ-bond metathesis reaction involving only a transition state rather than discrete ionic intermediates. A similar mechanism has been proposed in the reactions of $Cp^*_2ZrH_2$ with monofluoroarenes [19]. Other nucleophiles such as aryl and heteroaryl [31], alkyl [32], alkenyl [33], alkynyl [34], alkoxides, mercaptans, and amines [35] are well known to react with perfluorinated cyclic olefins to give substitution products by the same mechanism. These perfluorocycloolefins are highly toxic (similar to phosgene) as a result of their susceptibility to reactions with biological nucleophiles [36]. Similarly, $Cp^*_2ZrH_2$ mimics the vinylic H/F exchange chemistry observed in reactions of $LiAlH_4$ and $NaBH_4$ with perfluorinated cycloalkenes [37–39] further emphasizing the distinct hydridic character of $Cp^*_2ZrH_2$ [40].

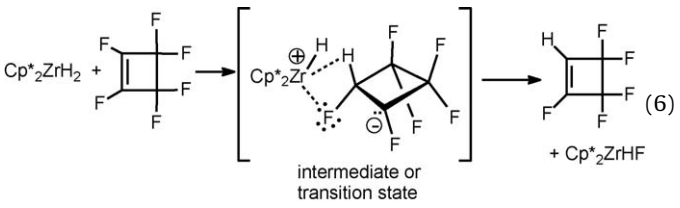

(6)

For all of the reactions studied involving **1** and cyclic perfluorinated olefins, the corresponding reactions with **2** give the same initial vinylic H/F exchanged products. However, unlike **1**, **2** does not easily react with any allylic C–F bonds of the cyclic olefins **B** and **G** [41] nor does **2** react further with any of the remaining C–F bonds of (*E*)-CFH=CFCF$_3$ [22]. It therefore appears that **2** is not readily capable of olefin insertion/β-F elimination, and may act only as a source of nucleophilic hydride. As previously reported, the non-perfluorinated olefins, 3,3,3-trifluoropropene and 1,1-difluoroethylene, are unreactive with **2** even with heating at 85 °C [21]. In addition, **2** does not undergo insertion with propene to afford $Cp^*_2Zr(n\text{-propyl})F$, suggesting that **2** is perhaps incapable of olefin insertion altogether.

These observations suggest that a change in the mechanism occurs when the olefin functionality is sufficiently less electrophilic as a result of decreased fluorination. For the cyclic perfluoroolefins, both vinylic H/F exchanges must occur before olefin insertion/β-F elimination will occur, as demonstrated by the regioselectivity of the exchange. With perfluoropropene, only one vinylic H/F exchange occurs readily at low temperature, and while this could be accommodated by either olefin insertion/β-F elimination or by hydride/fluoride exchange by σ-bond metathesis, DFT studies [22] indicated that the olefin insertion/β-F elimination pathway has a much lower barrier (<2 kcal mol^{-1}) than the hydride attack/fluoride elimination barrier (~7 kcal mol^{-1}), so that the former pathway is favored with this substrate. As this same conclusion is not possible with the cyclic perfluoroolefins, additional DFT studies were undertaken to elucidate the preferred mechanism for the H/F exchanges (vide infra).

The alternative mechanism involving insertion/α-F elimination, however, could be occurring if Cp^*_2ZrHF were able to react by insertion exclusively with perfluorinated olefins. For this reason, the insertion/α-F elimination mechanism cannot be discarded out of hand. Nevertheless, the hydride/fluoride σ-bond metathesis mechanism is favored based on the numerous precedents for this type of pathway, the similar reactivities of $Cp^*_2ZrH_2$ and $LiAlH_4$ toward perfluoroalkenes, the deficiency of solid evidence for α-fluoride elimination processes in zirconium, and lastly, the failure to observe any insertion intermediates.

2.6. Mechanistic considerations for the exchange of allylic C–F bonds

Regarding the subsequent allylic C–F activation reactions with **1** and dihydro-olefins **B** and **G** to give **C** and **H**, two mechanisms are considered: (1) hydride/fluoride σ-bond metathesis and (2) olefin insertion/β-F elimination. The former mechanism would involve hydride addition to generate a carbanion followed by fluoride elimination at the allylic position as before. However, the latter mechanism is supported by the following observations: Reaction of **1** with trifluoropropene gives observable insertion intermediates with formation of Zr–C bonds, **2** does not readily undergo insertion with other less electrophilic fluorinated olefins, such as olefins (*E*)-CFH=CFCF$_3$, CF$_2$=CHCF$_3$, **B**, and **G**, and lastly, **1** *does* react with olefins **B** and **G** to undergo allylic C–F activation.

2.7. Reaction of 1,4,4,5,5-pentafluorocyclopentene with $Cp^*_2ZrH_2$

Reaction of olefin **H** with **1** at room temperature produces complex **I** and H_2 in ~90% yield by NMR integration. Clearly, an insertion reaction does not occur with this olefin. The resistance to insertion may be reasoned using the electronic effects caused by fluorine substitution. By negative hyperconjugation arguments, olefin insertion is favored to place the hydride at the electron-deficient non-fluorinated vinylic carbon, and therefore disfavored at the fluorinated vinylic carbon (Fig. 2). However, attachment of

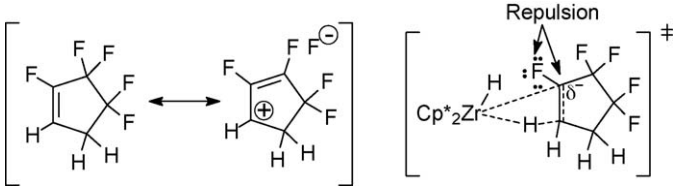

Fig. 2. The resistance of olefin **H** to undergo insertion into Zr–H is explained by negative hyperconjugation and electronic repulsion between the fluorine lone pairs and the developing negative charge on carbon.

hydride on the "favored" site would create a partial negative charge on the fluorine-substituted vinylic carbon in the transition state. Consequently, destabilizing repulsion between fluorine lone pairs and developing negative charge (I_π repulsion) occurs. The inability of an α-fluorine to stabilize a carbanionic intermediate is well established and is believed to outweigh the inductive stabilization by fluorine on the carbanion [42]. Consequently, an alternative pathway should be considered.

Vinylic C–H activation by the Zr^{II} complex, $[Cp^*_2Zr]_2(N_2)_3$, is well established [18]. The formation of **I** may therefore be explained by an associatively induced reductive elimination of H_2 to give an intermediate $Cp^*_2Zr^{II}$(olefin) complex followed by oxidative addition of the vinylic C–H bond (Eq. (7)). The reversibility of this process is supported by the observation of ~20% $Cp^*_2ZrH_2$ and olefin **H** in the ^1H NMR spectrum when complex **I** was heated at 100 °C in the presence of 1.3 atm H_2 for 1 day. In the absence of H_2, complex **I** remained stable at 120 °C.

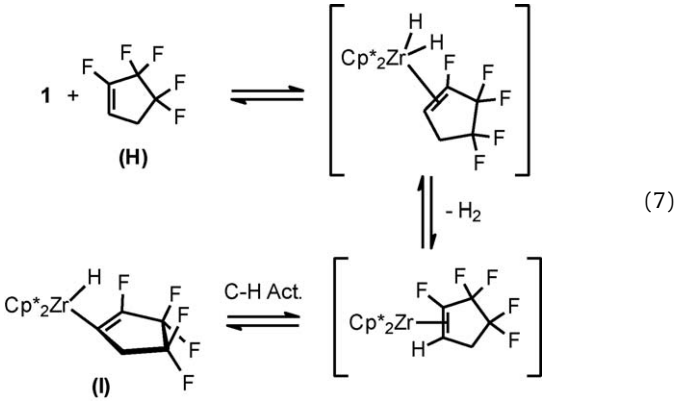

(7)

2.8. DFT calculations of C–F activation

As the above experimental investigations did not allow definitive determination of the mechanism of sp^2 C–F activation, we undertook DFT calculations of the mechanism for the first C–F activation. Cp_2ZrH_2 (**1′**, prime denotes Cp instead of Cp*) was considered as a model for **1** and both perfluorocyclobutene and perfluorocyclopentene were studied, as summarized in Figs. 3 and 4 and discussed below.

2.8.1. Perfluorocyclobutene

The formation of Cp_2ZrHF (**2′**) and 1,3,3,4,4-pentafluorocyclobutene through a σ-bond metathesis mechanism proceeds from a loose adduct, **4′**, between **1′** and perfluorocyclobutene. This adduct is more stable than the separated reactants on the potential energy surface ($\Delta E = -4.6$ kcal mol^{-1}), but entropy contributions render **4′** unstable on the Gibbs free energy surface ($\Delta G = +4.4$ kcal mol^{-1}). The Zr···F and H···C bond distances in **4′** are long (3.618 and 2.943 Å, resp.) and the geometry at the C=C double bond is planar, speaking against the description of **4′** as resulting from hydride nucleophilic attack. The situation is different in the transition state (TS) for hydride/fluoride σ-bond metathesis, **5′** (Fig. 5), where the C–F bond to be cleaved is significantly longer than the other vinylic C–F bond (1.369 Å vs. 1.325 Å). The C···H bond distance has also significantly reduced (1.756 Å) at the expense of the Zr–H bond (1.857 Å, **1′**; 1.905 Å, **5′**). The transition state **5′** can thus also be described as resulting from a nucleophilic attack from the hydride.

The transition state **5′** is only 0.7 kcal mol^{-1} above the separated reactants on the potential energy surface (ΔE), implying that there is no particular energy penalty associated with the metathesis. Indeed, the energy cost to perform the reaction is due to the loss of entropy associated with the increased order in the transition state, translating into an activation barrier $\Delta G^\ddagger = +13.9$ kcal mol^{-1}. The energetics for the σ-bond metathesis is rather similar to that obtained with perfluoropropene ($\Delta E^\ddagger = +2.2$ kcal mol^{-1}, $\Delta G^\ddagger = +15.5$ kcal mol^{-1}) [22]. As expected, once the transition state is surmounted, formation of a strong Zr–F bond in **2′** drives the thermodynamics of the transformation ($\Delta E = -73.5$ kcal mol^{-1}, $\Delta G = -72.0$ kcal mol^{-1}).

The adduct **4′** corresponds to a geometry where one vinylic C–F bond is pointing in between the two Zr–H bonds in **1′**. Another adduct, **6′**, was located on the potential energy surface where the C=C double bond is loosely interacting with the two hydrides

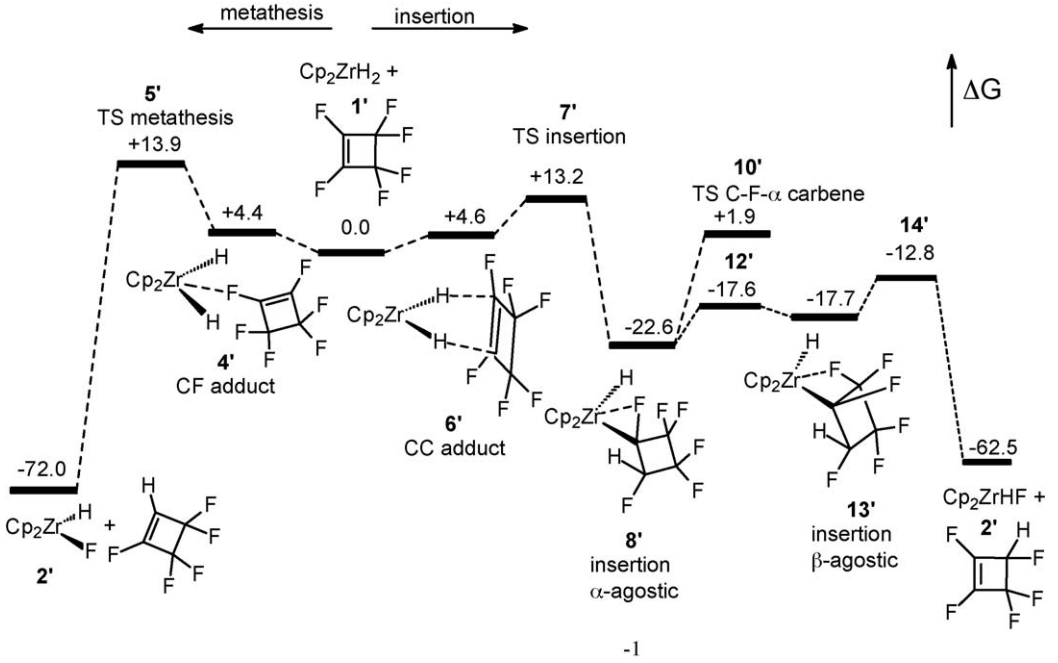

Fig. 3. Calculated free energy profiles (kcal mol^{-1}) for mechanisms of C-F activation of perfluorocyclobutene.

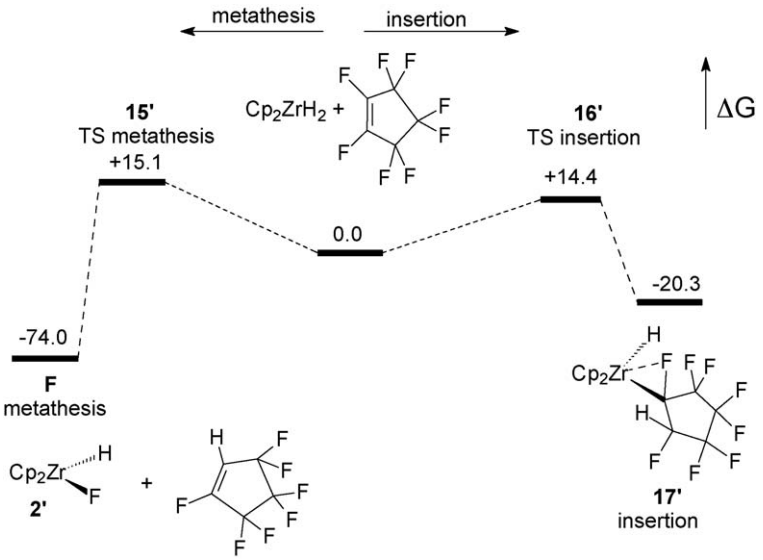

Fig. 4. Calculated free energy profiles (kcal mol^{-1}) for mechanisms of C–F activation of perfluorocyclopentene.

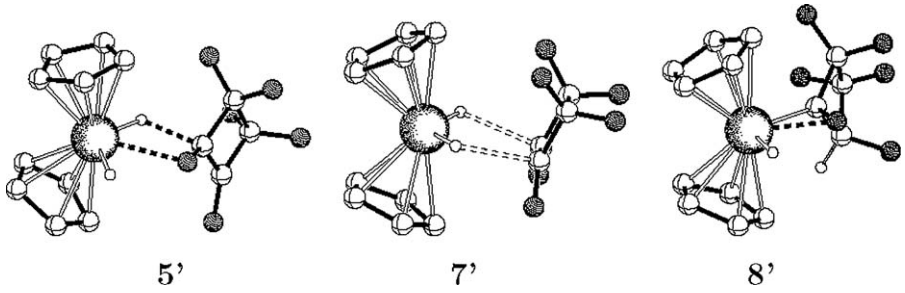

Fig. 5. Optimized geometries for the TS for σ-bond metathesis **5′**, the TS for olefin insertion **7′**, and the product of olefin insertion **8′**. H atoms on the Cp ligands have been omitted for clarity.

(ΔE = −4.8 kcal mol^{-1}, ΔG = +4.6 kcal mol^{-1}). The H···C bond distances are long (3.114 Å) and the C=C bond is unchanged compared to perfluorocyclobutene (1.341 Å). From this adduct, the TS for C=C insertion into one Zr–H bond, **7′** in Fig. 5, is reached with an energy of −2.3 kcal mol^{-1} with respect to separated reactants. This corresponds to an activation barrier $\Delta G^{\ddagger}$ = +13.2 kcal mol^{-1}. The essential geometrical features of TS **7′** are the shortening of the H···C bond distance (2.378 Å), the lengthening of the C=C bond (1.362 Å), and the opening of the H–Zr–H angle (112.6°, **1′**; 125.2°, **7′**). The product of insertion, **8′**, is a cyclobutyl complex featuring a C–F α-agostic interaction (C–F = 1.437 Å, Zr–C = 2.33 Å, Zr–C–F = 71.2°, see Fig. 5). **8′** is more stable than the separated reactants by 40.4 kcal mol^{-1} on the potential energy surface and by 22.6 kcal mol^{-1} on the Gibbs free energy surface.

In the case of perfluoropropene, the activation barrier was calculated to be $\Delta G^{\ddagger}$ = +12.0 kcal mol^{-1} vs. +15.5 kcal mol^{-1} for hydride/fluoride σ-bond metathesis. For perfluoropropene there was thus a clearer energy preference for olefin insertion over σ-bond metathesis ($\Delta\Delta G^{\ddagger}$ = +3.5 kcal mol^{-1}). In the case of perfluorocyclobutene, the difference is still in favor of olefin insertion but the difference is greatly reduced to $\Delta\Delta G^{\ddagger}$ = +0.7 kcal mol^{-1}. Moreover, the reduction of the difference originates from two effects: a lowering of $\Delta G^{\ddagger}$ for σ-bond metathesis and an increase of $\Delta G^{\ddagger}$ for insertion. This may result from a greater reactivity of perfluorocyclobutene toward hydride nucleophilic attack, and also, from a larger influence of steric bulk in the insertion process associated with the presence of the saturated part of the cyclobutene, which points towards the Cp ligand. The actual experimental system with Cp* instead of Cp would likely disfavor the insertion pathway more strongly with respect to the metathesis pathway due to increased steric interactions in transition state **7′** compared to transition state **5′**. To examine this possibility, transition states TS **5** and TS **7** were calculated relative to **1** and c-C_4F_6 using the full Cp* ligand rather than the Cp model ligand. The energies of these two transition states are indeed reversed, with the barrier to hydride/fluoride σ-bond metathesis ($\Delta G^{\ddagger}$ = + 20.7 kcal mol^{-1}) now being smaller than the barrier to insertion (+33.8 kcal mol^{-1}) by 13.1 kcal mol^{-1} [43]. This former barrier is small enough to easily be surmounted at room temperature ($\tau_{1/2} \sim 5$ min), as seen in the experiments.

From **8′**, the cis nature of the insertion reaction induces a geometry that prevents C–F β-elimination from the carbon atom where the hydride has been transferred. To generate **2′** and 1,3,3,4,4-pentafluorocyclobutene from **8′**, two pathways have been found. One possibility is to form directly the product through a 1,2 H-migration within the cyclobutyl ligand through the transition state **9′** (Fig. 6). The activation barrier from **8′** is computed to be $\Delta G^{\ddagger}$ = +38.1 kcal mol^{-1}. In **9′**, the C···F and Zr···C bonds are significantly elongated (C···F = 2.27 Å and Zr···C = 2.558 Å) and the migrating hydrogen is bridging two carbon atoms (C···H = 1.330 and 1.296 Å). The activation barrier through **9′** is larger than the value associated with the deinsertion reaction going back to the reactants **1′** and perfluorocyclobutene ($\Delta G^{\ddagger}$ = +35.8 kcal mol^{-1}). This rules out 1,2 migration as a potential pathway for the generation of the first defluorination product.

Another possibility is to generate a carbene intermediate by cleavage of the α-agostic C–F bond, this carbene yielding the final product by intramolecular H-migration. The transition state

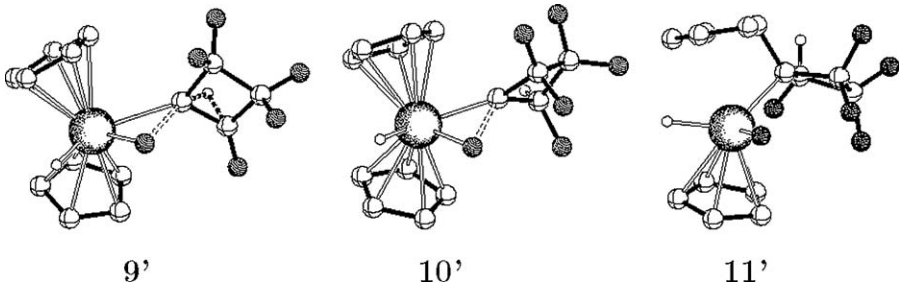

Fig. 6. Optimized geometries for the TS for H 1,2-migration **9′**, the TS for α-CF bond cleavage **10′**, and the product of α-CF bond cleavage **11′**. H atoms on the Cp ligands have been omitted for clarity.

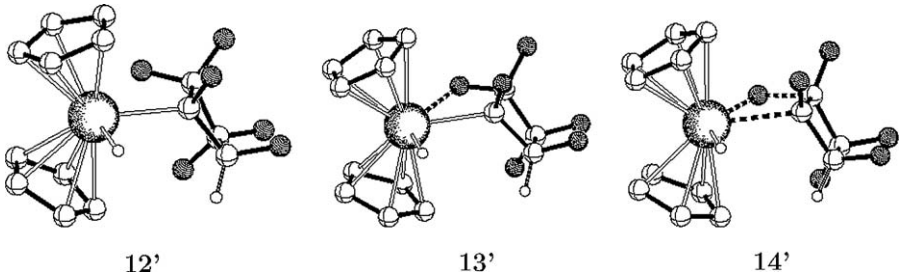

Fig. 7. Optimized geometries for the TS of rotation around Zr-C **12′**, the β-CF agostic intermediate **13′**, and the TS for β-CF cleavage **14′**. H atoms on the Cp ligands have been omitted for clarity.

associated with the cleavage of the α-agostic C–F bond, **10′**, is shown in Fig. 6. The activation barrier from **8′** ($\Delta G^{\ddagger}$ = 24.5 kcal mol^{-1}) is computed to be significantly lower than that for the 1,2 migration. In **10′**, the C–F bond is broken (C···F = 2.193 Å) and the Zr–C and Zr–F bonds are within bonding values (2.249 and 2.075 Å, resp.). The perturbation of the transition state geometry along the normal mode associated with the negative eigenvalue leads to **11′** where carbene is inserted between the metal and the Cp (Fig. 6). Even though **11′** is 24.2 kcal mol^{-1} more stable than **8′** on the Gibbs free energy surface, no attempt has been made to search for the pathway leading to **2′** and 1,3,3,4,4-pentafluorocyclobutene as a lower energy pathway from **8′** has been found.

From α-agostic complex **8′**, rotation around the Zr–C bond through TS **12′** yields a cyclobutyl intermediate **13′** featuring a β-agostic C–F bond (Fig. 7). The rotation is easy ($\Delta G^{\ddagger}$ = +5 kcal mol^{-1}) and the intermediate **13′** is marginally more stable (ΔG = −0.1 kcal mol^{-1}) than the TS **12′**. From **13′**, cleavage of the β-C–F bond is easy through TS **14′** ($\Delta G^{\ddagger}$ = +4.9 kcal mol^{-1}, see Fig. 7) to yield **2′** and 1,2,3,3,4-pentafluorocyclobutene with an overall Gibbs free energy of reaction of ΔG = −62.5 kcal mol^{-1}. Moreover, the highest barrier to overcome from **8′** is $\Delta G^{\ddagger}$ = +9.8 kcal mol^{-1} corresponding to the energy of TS **14′**, the transition state for β-C–F cleavage. This activation barrier is significantly lower than the activation barrier for cleavage of the α-agostic C–F bond via TS **10′** forming the carbene-like intermediate **11′**. Thus, if olefin insertion was to be the preferred pathway over the σ-bond metathesis, the product of allylic C–F activation should have been observed. This is not the result of the experimental observations and from the computational study it can safely be concluded that the first C–F activation proceeds through a σ-bond metathesis pathway for perfluorocyclobutene. The calculations also show that when olefin insertion is made possible, the activation of the allylic C–F bond is the preferred pathway. This pathway could account for the third H/F exchange.

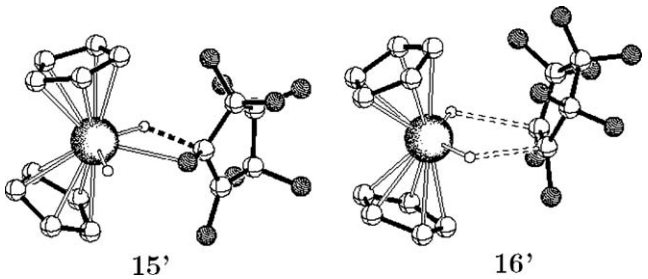

Fig. 8. Optimized geometries for the TS of σ-bond metathesis **15′**, and the TS for olefin insertion **16′**. H atoms on the Cp ligands have been omitted for clarity.

2.8.2. Perfluorocyclopentene

For the reaction of perfluorocyclopentene with **1′**, only the geometries of the TS for σ-bond metathesis **15′** and olefin insertion **16′** were optimized (Fig. 8). The activation barrier for σ-bond metathesis ($\Delta G^{\ddagger}$ = +15.1 kcal mol^{-1}) is slightly higher than for perfluorocyclobutene. The activation barrier for olefin insertion through **16′** is slightly lower ($\Delta G^{\ddagger}$ = +14.4 kcal mol^{-1}). Overall, there is still a slight preference for olefin insertion ($\Delta\Delta G^{\ddagger}$ = +0.7 kcal mol^{-1}) with the Cp_2Zr model compounds, but the difference is small enough to be reversed if the actual steric bulk of the Cp^* ligand is considered as seen with perfluorocyclobutene. Along the σ-bond metathesis pathway, the thermodynamics of the reaction with perfluorocyclopentene is similar to that with perfluorocyclobutene with ΔG = −74.0 kcal mol^{-1}. The product of olefin insertion **17′** features an α-agostic C–F bond interaction and is 20.3 kcal mol^{-1} more stable than the separated reactants on the Gibbs free energy surface. Therefore, this system is completely analogous to the perfluorocyclobutene system.

3. Conclusion

$Cp^*_2ZrH_2$ reacts with perfluorinated cycloolefins to give Cp^*_2ZrHF and vinylic H/F substituted organic products. A likely mechanism for this reaction based on DFT calculations is hydride/fluoride σ-bond metathesis. Cp^*_2ZrHF also reacts exclusively with vinylic C–F bonds of perfluorinated cyclic olefins to give $Cp^*_2ZrF_2$ and H/F exchanged organic products similar to those observed in reaction with $Cp^*_2ZrH_2$. Once both vinylic fluorines are replaced

with hydrogen, further hydrodefluorination proceeds by insertion/β-fluoride elimination. In contrast with $Cp^*_2ZrH_2$, allylic C–F bond activation is not observed using Cp^*_2ZrHF, suggesting that olefin insertion with non-perfluorinated olefins is extremely slow or non-existent with this complex.

4. Experimental

All manipulations were performed inside a N_2-filled Vacuum Atmospheres glovebox or on a high vacuum line. Cyclohexane, cyclohexane-d_{12}, and toluene-d_8 (Cambridge) were dried and vacuum distilled from purple solutions of benzophenone ketyl. UHP grade H_2 (Air Products) was purified by passage over activated 4 Å molecular sieves and MnO on vermiculite [44]. Perfluorocyclopentene (Matrix Scientific) and perfluorocyclobutene (PCR) were used as received. All liquids were degassed by the freeze-pump-thaw method. ^1H and ^{19}F NMR spectra were recorded using a Bruker Avance 400 spectrometer. ^{19}F NMR spectra were referenced to α,α,α-trifluorotoluene (taken as δ −63.73 relative to $CFCl_3$ with downfield chemical shifts taken to be positive). ^{19}F NMR spectra were recorded at a minimum resolution of 0.5 Hz. GC/MS analyses were conducted using a 5890A Series GC equipped with a Restek RTX-5 column (0.25 mm ID, 0.25 μm, 13 m) and a HP 5970 series mass selective detector. $Cp^*_2ZrH_2$ and $Hg(CF_3)_2$ were prepared according to the literature procedures [45,46]. *Caution*: Organomercury derivatives are highly poisonous and should be handled with great care [47]. *Warning*: Perfluorinated olefins are known to be highly toxic, volatile compounds [36]. The chemical shifts and coupling constants of the fluorinated olefins match those reported in the literature [48].

4.1. Reaction of 1 with perfluorocyclobutene

A resealable NMR tube was charged with 15 mg (0.041 mmol) of $Cp^*_2ZrH_2$ and dissolved in C_6D_{12}. The solution was freeze-pump-thaw degassed 3 times and with an 8.0-mL calibrated glass bulb, 95 Torr (0.041 mmol) of perfluorocyclobutene was condensed in the tube. The tube was thawed, shaken, and analyzed after 10 min. The starting olefin and $Cp^*_2ZrH_2$ were completely consumed. Cp^*_2ZrHF and $Cp^*_2ZrF_2$ were observed in 1:2.1 ratio. Two product olefins, 1,3,3,4,4-pentafluorocyclobutene (**A**) and 3,3,4,4-tetrafluorocyclobutene (**B**), were observed in 3.6:1 ratio. The volatiles of the reaction were transferred to an empty tube for ^{19}F COSY and GC/MS analysis. For **A**, ^1H NMR (C_6D_{12}): δ 5.73 (dd, J_{H-F} = 16.7 Hz, J_{H-F} = 9.4 Hz). ^{19}F NMR (C_6D_{12}): δ −105.1 (m, 1 F), −113.9 (m, 2 F), −118.7 (m, 2 F). GC/MS (*m*/*z*): 144 (M^+). For **B**, ^1H NMR (C_6D_{12}): δ 6.64 (m). ^{19}F NMR (C_6D_{12}): δ −111.2 (m). GC/MS (*m*/*z*): 127 (M^+). The solution contents were then transferred under vacuum into another NMR tube containing 13 mg $Cp^*_2ZrH_2$ (0.036 mmol) and analyzed 10 min later. Only olefins **B** and 1,4,4-trifluorocyclobutene (**C**) were observed in 1.9:1 ratio. For **C**, ^1H NMR (C_6D_{12}): δ 5.32 (m, 1 H), 2.48 (dm, J_{H-F} = 12.2 Hz, J_{H-H} = 3.1 Hz, 2 H). ^{19}F NMR (C_6D_{12}): δ −113.9 (d, *J* = 9.2 Hz, 2 F), −104.9 (s, 1 F). GC/MS (*m*/*z*): 108 (M^+). The volatiles were transferred onto more $Cp^*_2ZrH_2$ (16 mg, 0.044 mmol) and analyzed. Only **C**, the complex, $Cp^*_2Zr(c\text{-}C_4F_3H_2)H$ (**D**), and cyclobutane were observed in 17:4:1 ratio. H_2 was also observed at δ 4.54 in the ^1H NMR spectrum. For **D**, ^1H NMR (C_6D_{12}): δ 1.96 (s, Cp*, 30 H), 6.70 (s, Zr*H*, 1 H), the CH_2 group is obscured. ^{19}F NMR (C_6D_{12}): δ −98.4 (br s, 1 F), −111.9 (s, 2 F). For cyclobutane, ^1H NMR (C_6D_{12}): δ 1.95 (s). GC/MS (*m*/*z*): 56 (M^+).

4.2. Reaction of excess 1 with perfluorocyclobutene

A resealable NMR tube was charged with approximately 0.6 mL cyclohexane-d_{12} and 1.7 μL of α,α,α-trifluorotoluene. Perfluorocyclobutene (46 Torr, 0.018 mmol) was added on the vacuum line using a 7.4-mL calibrated glass bulb. The ^{19}F NMR spectrum revealed a 1.08: 1 mole ratio of perfluorocyclobutene: trifluorotoluene. $Cp^*_2ZrH_2$ (52 mg, 0.14 mmol) was added to the NMR tube and 1.3 atm H_2 was placed over the reaction mixture. The tube was heated for ∼8 h at 100 °C at which time analysis showed a few small (relative to trifluorotoluene) spurious fluorine resonances in the ^{19}F NMR spectrum. The volatiles of the reaction mixture were transferred under vacuum to an empty NMR tube. The ^1H NMR spectrum revealed a cyclobutane: trifluorotoluene mole ratio of 0.50:1, a 46% yield of cyclobutane.

4.3. Reaction of 1 with perfluorocyclopentene

A resealable NMR tube was charged with 12 mg (0.033 mmol) of $Cp^*_2ZrH_2$ and dissolved in C_6D_{12}. The solution was freeze-pump-thaw degassed 3 times and with an 8.0-mL calibrated glass bulb, 82 Torr (0.035 mmol) of perfluorocyclopentene was condensed in the tube. The tube was thawed, shaken, and analyzed after 10 min. Cp^*_2ZrHF and $Cp^*_2ZrF_2$ were observed in 10:1 ratio along with unreacted $c\text{-}C_5F_8$. Two product olefins, 1,3,3,4,4,5,5-heptafluorocyclopentene (**E**) and 1,2,3,3,4,5,5-heptafluorocyclopentene (**F**), were observed in 2.6:1 ratio. The volatiles of the reaction mixture were transferred under vacuum to an empty tube and reanalyzed by ^{19}F COSY and GC/MS. For **E**: ^{19}F NMR (C_6D_{12}): δ −105.8 (d, *J* = 12 Hz, 2 F), −119.2 (m, 2 F), −123.5 (m, 1 F), −129.3 (m, 2 F). ^1H NMR (C_6D_{12}): δ 5.77 (m). GC/MS (*m*/*z*): 194 (M^+). For **F**: ^{19}F NMR (C_6D_{12}): δ −110.9 (dm, $J_{gem\ F-F}$ = 203 Hz, 2 F), −128.3 (dm, $J_{gem\ F-F}$ = 203 Hz, 2 F), −201.6 (m, 2 F), −204.6 (m, 1 F). ^1H NMR (C_6D_{12}): δ 5.67 (dm, $J_{gem\ H-F}$ = 62 Hz). GC/MS (*m*/*z*): 194 (M^+). The contents of the tube were transferred under vacuum onto another 12 mg (0.033 mmol) of $Cp^*_2ZrH_2$, thawed, shaken, and analyzed after 5 min at room temperature. Again, Cp^*_2ZrHF and a trace of $Cp^*_2ZrF_2$ were observed. Olefins **E**, **F**, 3,3,4,4,5,5-hexafluorocyclopentene (**G**), and 1,4,4,5,5-pentafluorocyclopentene (**H**), were observed in 17.8:6.7:1.4:1 ratio. The volatiles were transferred under vacuum into an empty tube and analyzed by ^{19}F COSY and GC/MS. For **G**: ^{19}F NMR (C_6D_{12}): δ −108.9 (m, 4 F), −131.5 (quin, 2 F). ^1H NMR (C_6D_{12}): δ 6.33 (m). GC/MS (*m*/*z*): 176 (M^+). For **H**: ^{19}F NMR (C_6D_{12}): δ −113.8 (m, 2 F), −120.8 (dm, *J* = 14.3 Hz, 2 F), −135.0 (m, 1 F). ^1H NMR (C_6D_{12}): δ 5.46 (m, 1 H), 2.67 (m, 2 H). GC/MS (*m*/*z*): 158 (M^+). Treatment of this mixture twice more with 12 mg portions of $Cp^*_2ZrH_2$ and allowing to stand at room temperature produced an olefin mixture containing **H**, **G**, **F**, and **E** in 16:1:2:4.6 ratio. A small amount of an unidentified species was also observed. Treatment with 15 mg $Cp^*_2ZrH_2$ again and allowing to stand at room temperature for 40 min produced ∼80% olefin **H**. Further characterization of **H** was accomplished by hydrogenation over 10% Pd on carbon over 20 min in C_6D_{12} solution to produce 1,1,2,2,3-pentafluorocyclopentane. ^{19}F NMR (C_6D_{12}): δ −112.9 (dm, J_{F-F} = 246 Hz, 1 F), −116.1 (dm, J_{F-F} = 246 Hz, 1 F), −125.6 (dm, $J_{gem\ F-F}$ = 257 Hz, 1 F), −135.1 (dm, $J_{gem\ F-F}$ = 257 Hz, 1 F), −196.33 (m, 1 F). ^1H NMR (C_6D_{12}): δ 4.73 (dm, J_{H-F} = 52 Hz, 1 H), 2.30 (m, 1 H), 2.08 (m, 2 H), 2.04 (m, 1 H).

4.4. Reaction of 1 with c-C_5F_8 in the presence of triphenylmethane

A resealable NMR tube was charged with $Cp^*_2ZrH_2$ (10 mg, 0.027 mmol) and triphenylmethane (67 mg, 0.27 mmol) and dissolved in C_6D_{12}. Using an 8.0-mL calibrated glass bulb, perfluorocyclopentene (63 Torr, 0.027 mmol) was condensed into the tube and warmed to room temperature. Olefins **E** and **F** were observed in 2.7:1 ratio.

4.5. Reaction of Cp^*_2ZrHF with c-C_4F_6 and c-C_5F_8

A resealable NMR tube was charged with Cp^*_2ZrHF (16 mg, 0.042 mmol) and dissolved in C_6D_{12}. Using an 8.0-mL calibrated

glass bulb, perfluorocyclobutene (95 Torr, 0.041 mmol) was condensed in the tube. After 2 h at room temperature, the reaction was complete, forming $Cp^*_2ZrF_2$ and olefin **A** in ~ 90% yield. The same procedure was repeated using perfluorocyclopentene (95 Torr, 0.041 mmol). The reaction was complete after 1 day at room temperature to give $Cp^*_2ZrF_2$ and olefin **E** in ~ 95% yield.

4.6. Synthesis of $Cp^*_2Zr(c\text{-}C_5F_5H_2)H$/$Cp^*_2Zr(c\text{-}C_5F_5H_2)Cl$

400 mg $Cp^*_2ZrH_2$ (1.10 mmol) was weighed into an ampule. Approximately 4 mL of cyclohexane was transferred under vacuum into the flask. Using an 8.0-mL calibrated glass bulb, 520 Torr (0.225 mmol) perfluorocyclopentene was condensed into the flask. The solution was warmed to room temperature. After stirring for 3 d, 600 Torr anhydrous HCl (0.26 mmol, 8-mL volume) was condensed into the ampule and heated in an 80 °C oil bath for 1 day. The ampule was freeze-pump-thaw degassed 5 times using an acetone/dry ice bath to remove most of the excess HCl. Final traces of HCl were removed by vacuum transferring the volatiles of the mixture onto 40 mg $Cp^*_2ZrH_2$ and quickly transferring the volatiles again into an empty ampule. ^{19}F NMR analysis of this solution showed 1,4,4,5,5-pentafluorocyclopentene (**H**) and only a trace of a single unidentified impurity. To this mixture, 1.0 μL of α,α,α-trifluorotoluene was added and analyzed by ^{19}F NMR to calculate the amount of olefin present in solution.

In a small flask, $Cp^*_2ZrH_2$ (45 mg, 0.124 mmol) was added and dissolved with the 1,4,4,5,5-pentafluorocyclopentene/C_6H_{12} solution (containing 0.12 mmol olefin) prepared above. The solution was stirred for 3 d at room temperature producing a 10:1 mixture of $Cp^*_2Zr(c\text{-}C_5F_5H_2)H$ (**I**) and Cp^*_2ZrHF by ^{19}F NMR integration. The product was purified by crystallization from pentane at −30 °C to yield 49 mg (42%) of analytically pure material. For **I**: ^{19}F NMR (toluene-d_8): δ −113.5 (m, 2 F), −120.1 (d, 2 F), −129.63 (t, 1 F). ^1H NMR (toluene-d_8): δ 6.59 (s, Zr*H*, 1 H), 1.76 (s, Cp*, 30 H), 2.37 (m, 2 H). Anal. calcd for $C_{25}H_{33}ZrF_5$: C, 57.77; H, 6.40. Found: C, 57.61; H, 6.47. Treatment of $Cp^*_2Zr(c\text{-}C_5F_5H_2)H$ with anhydrous HCl at room temperature leads to quantitative formation of $Cp^*_2Zr(c\text{-}C_5F_5H_2)Cl$ (**J**). For **J**: ^{19}F NMR (toluene-d_8): δ −115.2 (m, 2 F), −121.7 (dm, J_{F-F} = 18.7 Hz, 2 F), −124.3 (tm, J_{F-F} = 18.5 Hz, 1 F). ^1H NMR (toluene-d_8): δ 1.71 (s, Cp*, 30 H), 2.77 (m, 2 H). Anal. calcd for $C_{25}H_{32}ZrF_5Cl$: C, 54.18; H, 5.82. Found: C, 54.47; H, 5.79. **J** was crystallized from pentane at −30 °C for X-ray analysis.

4.7. Reaction of 1 with $Hg(CF_3)_2$

A resealable NMR tube was charged with $Cp^*_2ZrH_2$ (15 mg, 0.041 mmol) and $Hg(CF_3)_2$ (3 mg, 0.009 mmol) followed by addition of C_6D_{12} at room temperature. Evolution of H_2 and Hg^0 were observed. ^1H NMR analysis revealed the presence of **2**, $Cp^*_2ZrF_2$, and small amounts of CH_3F, CH_4, and CH_3CH_3. ^1H NMR (C_6D_{12}): δ 4.08 (d, J_{H-F} = 48 Hz, CH_3F), δ 0.18 (s, CH_4), δ 0.85 (s, CH_3CH_3).

4.8. Reaction of 1 with $Hg(CF_3)_2$ in the presence of tetramethylethylene

A resealable NMR tube was charged with $Cp^*_2ZrH_2$ (12 mg, 0.033 mmol) and dissolved in toluene-d_8 followed by addition of tetramethylethylene (39 μL, 0.33 mmol) via syringe. Solid $Hg(CF_3)_2$ (5 mg, 0.015 mmol) was added to the NMR tube, closed, and shaken at room temperature. Evolution of H_2 and Hg^0 were observed. The sample was degassed at −78 °C and the remaining volatiles were transferred under vacuum into an empty NMR tube. NMR analysis of this sample revealed the presence of 1-fluoro-2,2,3,3-tetramethylcyclopropane in 54% yield [49]. No CH_3F was observed when the reaction was performed in the presence of the carbene trap. For $C_7H_{13}F$: ^1H NMR (C_6D_{12}): δ 3.67 (d, 1 H, J_{H-F} = 66 Hz), 1.02 (d, 6 H, J = 1.4 Hz), 0.76 (d, 6 H, J = 2.7 Hz). ^{19}F NMR: δ −223.5 (dm, J_{H-F} = 66 Hz). GC/MS (m/z): 116 (M^+).

4.9. Computational details

All calculations were performed with the Gaussian03 package [50] within the framework of Density Functional Theory using the hybrid functional B3PW91 [51]. The zirconium atom was represented by the relativistic effective core potential (RECP) from the Stuttgart group (12 valence electrons) and the associated basis set [52], augmented by an f polarization function [53]. The remaining atoms (C, H, F) were represented by a 6-31G(d,p) basis set [54]. Full optimizations of geometry without any constraint were performed followed by analytical computation of the Hessian matrix to confirm the nature of the located extrema as minima or transition states on the potential energy surface. Connection between reactants and products through a given transition state was checked by optimizing as a minimum a slightly altered geometry of the TS along both directions of the TS vector.

A CIF for compound **J** has been deposited with the Cambridge Crystallographic Data Centre, as CCDC #771381. A copy of this information may be obtained free of charge from The Director, CCDC, 12 Union Road, Cambridge CB2 1EZ, UK. Fax. (int. code) +44 1223 336 033 or Email: deposit@ccdc.cam.ac.uk or http://www.ccdc.cam.ac.uk.

Acknowledgments

The U.S. Department of Energy, Grant FG02-86ER13569 is gratefully acknowledged for their support of this work. E.C and O.E. thank the CNRS and the Ministère of High Education and Research for funding.

Appendix A. Supplementary data

Supplementary data associated with this article can be found, in the online version, at doi:10.1016/j.jfluchem.2010.05.003.

References

[1] H. Amii, K. Uneyama, Chem. Rev. 109 (2009) 2119.
[2] T. Braun, R.N. Perutz, Chem. Commun. (2002) 2749.
[3] M.K. Whittlesey, R.N. Perutz, M.H. Moore, Chem. Commun. (1996) 787; M.K. Whittlesey, R.N. Perutz, B. Greener, M.H. Moore, Chem. Commun. (1997) 187.
[4] S. Hintermann, P.S. Pregosin, H. Rüegger, H.C. Clark, J. Organomet. Chem. 435 (1992) 225.
[5] B.L. Edelbach, W.D. Jones, J. Am. Chem. Soc. 119 (1997) 7734.
[6] P.K. Chan, W.K. Leong, Organometallics 27 (2008) 1247.
[7] (a) L. Cronin, C.L. Higgitt, R. Karch, R.N. Perutz, Organometallics 16 (1997) 4920; (b) T. Braun, S.P. Foxon, R.N. Perutz, P.H. Walton, Angew. Chem., Int. Ed. 38 (1999) 3326; (c) T. Braun, M.I. Sladek, R.N. Perutz, Chem. Commun. (2001) 2254; (d) M.I. Sladek, T. Braun, B. Neumann, H.-G. Stammler, Dalton Trans. (2002) 297; (e) M. Reinhold, J.E. McGrady, R.N. Perutz, J. Am. Chem. Soc. 126 (2004) 5268.
[8] S.T. Belt, M. Helliwell, W.D. Jones, M.G. Partridge, R.N. Perutz, J. Am. Chem. Soc. 115 (1993) 1429.
[9] R.P. Hughes, R.T. Carl, S.J. Doig, R.D. Hemond, D.E. Samkoff, W.L. Smith, L.C. Stewart, R.E. Davis, K.D. Holland, P. Dickens, R.P. Kashyap, Organometallics 9 (1990) 2732.
[10] H.C. Clark, J.H. Tsai, Inorg. Chem. 5 (1966) 1407.
[11] (a) Y.Z. Huang, J. Li, J. Zhou, Z. Zhu, G. Hou, J. Organomet. Chem. 205 (1981) 185; (b) Y.Z. Huang, J. Li, J. Zhou, Q. Wang, M. Gui, J. Organomet. Chem. (1981) 169.
[12] B.E. Smart, in: S. Patai, Z. Rappoport (Eds.), The Chemistry of Functional Groups, Supplement D, John Wiley & Sons, New York, 1983, , Chapter 14.
[13] P.M. Treichel, J. Morris, F.G.A. Stone, J. Chem. Soc. (1963) 720.
[14] P.M. Treichel, E. Pitcher, F.G.A. Stone, Inorg. Chem. 1 (1962) 511.
[15] (a) T. Braun, D. Noveski, B. Neumann, H.-G. Stammler, Angew. Chem., Int. Ed. 41 (2002) 2745; (b) D. Noveski, T. Braun, M. Schulte, B. Neumann, H.-G. Stammler, Dalton Trans. (2003) 4075.
[16] M.S. Kirkham, M.F. Mahon, M.K. Whittlesey, Chem. Commun. (2001) 813.

[17] M.F. Kühnel, D. Lentz, Angew. Chem., Int. Ed. Engl. 49 (2010) 2933.
[18] B.M. Kraft, R.J. Lachicotte, W.D. Jones, J. Organomet. Chem. 658 (2002) 132.
[19] (a) B.M. Kraft, R.J. Lachicotte, W.D. Jones, J. Am. Chem. Soc. 122 (2000) 8559;
(b) B.M. Kraft, R.J. Lachicotte, W.D. Jones, J. Am. Chem. Soc. 123 (2001) 10973.
[20] B.M. Kraft, R.J. Lachicotte, W.D. Jones, Organometallics 21 (2002) 727.
[21] B.M. Kraft, R.J. Lachicotte, W.D. Jones, J. Am. Chem. Soc. 124 (2002) 8681.
[22] E. Clot, C. Mégret, B.M. Kraft, O. Eisenstein, W.D. Jones, J. Am. Chem. Soc. 126 (2004) 5647.
[23] W.D. Jones, J. Chem. Soc., Dalton Trans. (2003) 3991.
[24] Y.V. Zeifman, E.G. Ter-Gabrielyan, N.P. Gambaryan, I.L. Knunyants, Russ. Chem. Rev. 53 (1984) 256.
[25] J.F. Hartwig, Organotransition Metal Chemistry from Bonding to Catalysis, University Science Books, Sausalito, California, 2010, p. 366.
[26] Several reports of β-fluoride elimination show cis-elimination transition states. See:
S.A. Strazisar, P.R. Wolczanski, J. Am. Chem. Soc. 123 (2001) 4728;
A. Paul, A.J. Gellman, Langmuir 11 (1995) 4433;
A.R. Fout, J. Scott, D.L. Miller, B.C. Bailey, M. Pink, D.J. Mindiola, Organometallics 29 (2009) 331;
D. Huang, K.B. Renkema, K.G. Caulton, Polyhedron 25 (2006) 459;
In particular the report by Wolczanski looked at a series of Ta–CH_2CH_2X β-eliminations and demonstrated cis-β-elimination in ethoxyethyl ethers. Late metals, however, with electrons available to displace β-fluoride as F^- can undergo trans-eliminations. See:
C.J. Bourgeois, R.P. Hughes, J. Yuan, A.G. DiPasquale, A.L. Rheingold, Organometallics 25 (2006) 2908.
[27] Mercury reagents have been effective for the stoichiometric synthesis of fluoroaryl hydride derivatives of $Cp^*_2ZrH_2$. See Ref. 19b.
[28] M. Kamel, W. Kimpenhaus, J. Buddrus, Chem. Ber. 109 (1976) 2351, $Cp^*_2ZrH_2$ is unreactive with tetramethylethylene even with heating at 85 °C..
[29] J.A. Morrison, Adv. Organomet. Chem. 35 (1993) 211.
[30] F.L. Taw, B.L. Scott, J.L. Kiplinger, J. Am. Chem. Soc. 125 (2003) 14712.
[31] T. Yamaguchi, M. Irie, J. Org. Chem. 70 (2005) 10323;
M. Frigoli, G.H. Mehl, Chem. Eur. J. 10 (2004) 5243;
M. Giraud, A. Leaustic, M.-F. Charlot, P. Yu, M. Cesario, C. Philouze, R. Pansu, K. Nakatani, E. Ishow, New J. Chem. 29 (2005) 439;
K. Higashiguchi, K. Matsuda, N. Tanifuji, M. Irie, J. Am. Chem. Soc. 127 (2005) 8922;
Y. Yokoyama, H. Shiraishi, Y. Tani, Y. Yokoyama, Y. Yamaguchi, J. Am. Chem. Soc. 125 (2003) 7194.
[32] R.D. Chambers, J.R. Kirk, R.L. Powell, J. Chem. Soc., Perkin Trans. 1 (1983) 1239.
[33] A. Peters, C. Vitols, R. McDonald, N.R. Branda, Org. Lett. 5 (2003) 1183.
[34] S. Yamada, T. Konno, T. Ishihara, H. Yamanaka, J. Fluorine Chem. 126 (2005) 125.
[35] R.D. Chambers, M.P. Greenhall, J. Fluorine Chem. 107 (2001) 171.
[36] C.M. Timperley, J. Fluorine Chem. 125 (2004) 685.
[37] W.J. Feast, D.R.A. Perry, R. Stephens, Tetrahedron 22 (1966) 433.
[38] D.J. Burton, R.L. Johnson, Tetrahedron Lett. 7 (1966) 2681.
[39] G. Fuller, J.C. Tatlow, J. Chem. Soc. (1961) 3198.
[40] J.E. Bercaw, Adv. Chem. Ser. 167 (1978) 136.
[41] Although olefin **B** was unreactive with Cp^*_2ZrHF at 80 °C after 3 hours, olefin **G** did react to give olefin **H**, but only very slowly (~30% conversion after 1 week at 80 °C in the presence of 1 equiv of Cp^*_2ZrHF).
[42] R.E. Banks, B.E. Smart, J.C. Tatlow (Eds.), Organofluorine Chemistry: Principles and Commercial Applications, Plenum Press, New York, 1994.
[43] The steric influence on these barriers may be overestimated, as dispersion forces (attractive van der Waals forces) are not well represented with the functional used here. The influence of the methyl groups on the cyclopentadienyl ligand on the energy barriers or reaction energies should only be considered qualitatively because steric repulsion is partly compensated by dispersion forces. The functional used in this work is unable to represent weak interactions, as shown in Y. Zhao, D.G. Truhlar, Acc. Chem. Res. 41 (2008) 157. Such calculations are beyond the focus of this paper.
[44] T.L. Brown, D.W. Dickerhoof, D.A. Bafus, G.L.D. Morgan, Rev. Sci. Instrum. 22 (1962) 491.
[45] L.E. Schock, T.J. Marks, J. Am. Chem. Soc. 110 (1988) 7701.
[46] R. Eujen, Inorg. Synth. 24 (1986) 52.
[47] M.B. Blayney, J.S. Winn, D.W. Nierenberg, Chem. Eng. News 75 (1997) 7.
[48] H. Koroniak, K.W. Palmer, W.R. Dolbier, H. Zhang, Mag. Res. Chem. 31 (1993) 748.
[49] D.J. Burton, J.L. Hahnfeld, J. Org. Chem. 42 (1977) 828.
[50] M.J. Frisch, G.W. Trucks, H.B. Schlegel, G.E. Scuseria, M.A. Robb, J.R. Cheeseman, J.A. Montgomery Jr., T. Vreven, K.N. Kudin, J.C. Burant, J.M. Millam, S.S. Iyengar, J. Tomasi, V. Barone, B. Mennucci, M. Cossi, G. Scalmani, N. Rega, G.A. Petersson, H. Nakatsuji, M. Hada, M. Ehara, K. Toyota, R. Fukuda, J. Hasegawa, M. Ishida, T. Nakajima, Y. Honda, O. Kitao, H. Nakai, M. Klene, X. Li, J.E. Knox, H.P. Hratchian, J.B. Cross, V. Bakken, C. Adamo, J. Jaramillo, R. Gomperts, R.E. Stratmann, O. Yazyev, A.J. Austin, R. Cammi, C. Pomelli, J.W. Ochterski, P.Y. Ayala, K. Morokuma, G.A. Voth, P. Salvador, J.J. Dannenberg, V.G. Zakrzewski, S. Dapprich, A.D. Daniels, M.C. Strain, O. Farkas, D.K. Malick, A.D. Rabuck, K. Raghavachari, J.B. Foresman, J.V. Ortiz, Q. Cui, A.G. Baboul, S. Clifford, J. Cioslowski, B.B. Stefanov, G. Liu, A. Liashenko, P. Piskorz, I. Komaromi, R.L. Martin, D.J. Fox, T. Keith, M.A. Al-Laham, C.Y. Peng, A. Nanayakkara, M. Challacombe, P.M.W. Gill, B. Johnson, W. Chen, M.W. Wong, C.J.A. Gonzalez, Gaussian 03, Revision C. 02, Pople, Gaussian, Inc., Wallingford, CT, 2004.
[51] (a) A.D. Becke, J. Chem. Phys. 98 (1993) 5648;
(b) J.P. Perdew, Y. Wang, Phys. Rev. B 45 (1992) 13244.
[52] D. Andrae, U. Haüssermann, M. Dolg, H. Stoll, H. Preuss, Theor. Chim. Acta 77 (1990) 123.
[53] A.W. Ehlers, M. Böhme, S. Dapprich, A. Gobbi, A. Höllwarth, V. Jonas, K.F. Köhler, R. Stegmann, A. Veldkamp, G. Frenking, Chem. Phys. Lett. 208 (1993) 111.
[54] P.C. Hariharan, J.A. Pople, Theor. Chim. Acta 28 (1973) 213.